Strategies for braiding and ground state preparation in digital quantum hardware

Herasymenko, Y.

3 Electrical detection of the Majorana fusion rule for chiral edge vortices in a topological superconductor

3.1 Introduction

Vortices in a two-dimensional topological superconductor contain a midgap state, or *zero-mode*, that can be used to store quantum mechanical information in a nonlocal way, protected from local sources of decoherence [3, 4, 78, 112, 113]. The qubit degree of freedom is the fermion parity of any two widely separated vortices, which may or may not share an unpaired electron or hole (a fermionic quasiparticle) in the condensate of Cooper pairs. The pairwise exchange, or *braiding*, of vortices is a unitary transformation which can serve as a building block for a quantum computation [32, 114]. The merging, or *fusion*, of two vortices is the read-out operation [115]: The qubit is in the state $|1\rangle$ or $|0\rangle$ depending on whether or not the vortices leave behind a unpaired fermion. The fact that braiding operations do not commute, referred to as *non-Abelian statistics*, goes hand-in-hand with the fact that the fusion outcome is non-deterministic. As illustrated in Fig. 3.1, the fusion of two vortices σ produces a quantum superposition of states ψ and $\mathbb{I}$ with and without a quasiparticle excitation. This is the Majorana fusion rule* of non-Abelian anyons, symbolically written as $\sigma \otimes \sigma = \psi \oplus \mathbb{I}$.

Neither the braiding nor the fusion of vortices has been realized in the laboratory. This has motivated a variety of theoretical proposals for methods to demonstrate the appearance of non-Abelian anyons in a topological superconductor [90–93]. The obstacle that these proposals seek to remove, is the need to physically move the zero-modes around. Ref. [116] proposes an alternative approach: Substitute immobile bulk

*Because of a mapping onto the Ising model, the term "Ising fusion rule" is also used.

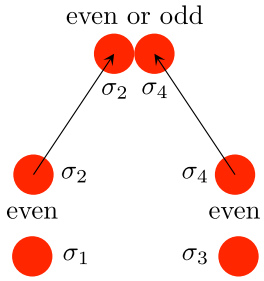

Figure 3.1: Schematic illustration of the fusion rule $\sigma_2 \otimes \sigma_4 = \psi \oplus \mathbb{I}$ of Majorana zero-modes (red dots, labeled σ_n). Pairs of zero-modes may or may not share a quasiparticle. In the former case the fermion parity is "odd" (indicated by ψ), in the latter case it is "even" (indicated by $\mathbb{I}$). The overall fermion parity is conserved, so if the fusion of σ_2 and σ_4 leaves behind a quasiparticle, then the fusion of σ_1 and σ_3 must also produce a quasiparticle.

vortices for mobile edge vortices. In that paper the braiding of vortices was considered. Here we turn to the fusion of edge vortices, in order to demonstrate the Majorana fusion rule.

Edge vortices are π-phase domain walls for Majorana fermions propagating along the edge of a topological superconductor [102]. Edge vortices may appear stochastically from quantum phase slips at a Josephson junction [95–97], but for our purpose we use the *deterministic* injector of Ref. [116]: A voltage pulse $V(t)$ of integrated magnitude $\int V(t)dt = h/2e$ applied over a Josephson junction injects an edge vortex at each end of the junction. The injection happens when the phase difference ϕ of the superconducting pair potential crosses π. At $\phi = \pi$ the effective gap $\Delta_0 \cos(\phi/2)$ in the junction changes sign [25]. By the same mechanism that is operative in the Kitaev chain [86], the gap inversion creates a zero-mode at each end of the junction, which then propagates away from the junction along the edge mode. The edge modes are chiral, meaning that the motion is in a single direction only. For our purpose we need that the propagation is in the same direction along both edges connected by a Josephson junction. The geometry of Fig. 3.2 shows one way to achieve this using a topological insulator/magnetic insulator/superconductor heterostructure [94, 99]. (In Fig. 3.3 we show an alternative realization using a Chern insulator/superconductor heterostructure [27, 98].)

In the next section 3.2 we describe the way in which the fusion process shown schematically in Fig. 3.1 can be implemented in the structure of Figs. 3.2 and 3.3. In the subsequent sections 3.3 and 3.4 we present an

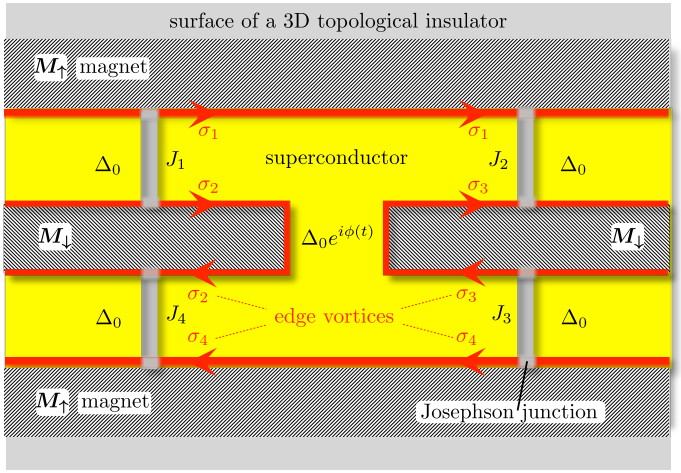

Figure 3.2: Geometry to create and fuse two pairs of edge vortices in a topological insulator/magnetic insulator/superconductor heterostructure. The edge vortices are created at Josephson junctions J_1 and J_3, by a 2π increment of the superconducting phase $\phi(t)$ on the central superconducting island. Each edge vortex contains a Majorana zero-mode and two zero-modes define a fermion parity qubit. The initial state $|J_1 J_3\rangle = |00\rangle$ has even-even fermion parity. When the edge vortices fuse at Josephson junctions J_2 and J_4 the final state $|J_2 J_4\rangle = (|00\rangle + i|11\rangle)/\sqrt{2}$ is in an equal-weight superposition of even-even and odd-odd parity states.

explicit calculation of the fermion parity of the final state, to demonstrate the equal-weight superposition of even and odd fermion parity implied by the Majorana fusion rule. Sec. 3.5 addresses an electrical signature of the fusion process: The sum $I_\mathrm{L} + I_\mathrm{R}$ of the currents at the two ends of the structure shows shot noise, because of the nondeterministic nature of the fusion process, but the difference $I_\mathrm{L} - I_\mathrm{R}$ is nearly noiseless, because of the correlated fermion parity. We conclude in Sec. 3.6.

3.2 Edge vortex injection and fusion in a four-terminal Josephson junction

The geometry of Fig. 3.2, with four incoming and four outgoing Majorana edge modes was introduced in Ref. [117] and studied recently in Refs. [33, 118, 119]. Those earlier works considered the injection of *fermions*:

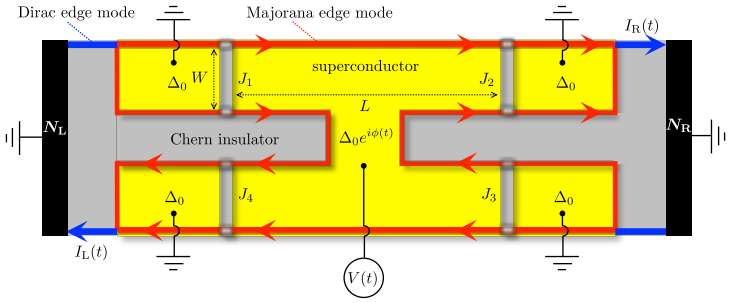

Figure 3.3: Same as Fig. 3.2, but now in a Chern insulator/superconductor heterostructure with normal metal contacts (N_L, N_R) to detect the charge produced upon fusion of the edge vortices. An integrated voltage pulse $\int V(t)dt = h/2e$ induces a 2π phase shift over the four Josephson junctions J_1, J_2, J_3, J_4, which results in a current pulse $I_L(t)$, $I_R(t)$ into the left and right contact. While I_L and I_R separately, as well as the sum $I_L + I_R$, exhibit shot noise, the difference $I_L - I_R$ becomes exactly noiseless for identical junctions J_1 and J_3.

electrons and holes injected into the Majorana edge modes from a normal metal contact. Here instead we consider the injection of *vortices*: π-phase domain walls injected into the edge modes by a Josephson junction. The injection happens in response to a voltage pulse $\int V(t)dt = h/2e$, which advances by 2π the phase $\phi(t)$ of the pair potential $\Delta_0 e^{i\phi}$. (Alternatively, an $h/2e$ flux bias achieves the same.) If the width W of the Josephson junction is large compared to the superconducting coherence length $\xi_0 = \hbar v_F/\Delta_0$, the injection happens in a short time interval $t_\phi \simeq (\xi_0/W)\Delta t$ around $\phi(t) = \pi$, short compared the duration Δt of the voltage pulse [116].*

The edge vortices σ_n are anyons with a non-Abelian exchange statistics encoded in the Clifford algebra of Majorana operators γ_n,

$$\gamma_n\gamma_m + \gamma_m\gamma_n = \delta_{nm}. \tag{3.2.1}$$

Each edge vortex has a zero-mode and two zero-modes n, m encode a qubit degree of freedom in the fermion parity $P_{nm} = 2i\gamma_n\gamma_m$ with eigenvalues ± 1. Provided the vortices are non-overlapping, the qubit is protected from local sources of decoherence.

In the four-terminal Josephson junction of Fig. 3.2, one pair of edge vortices σ_1, σ_2 is injected at Josephson junction J_1 and a second pair

*This separation of time scales $t_\phi/\Delta t \simeq \xi_0/W \ll 1$ is why it is meaningful to distinguish the injection of vortices from the injection of fermions, since a Majorana fermion in an edge mode is equivalent to a pair of overlapping edge vortices.

σ_3, σ_4 is injected at Josephson junction J_3. Because the voltage pulse cannot create an unpaired fermion, the edge vortices are injected in a state $|\Psi\rangle$ of even fermion parity, $P_{12}|\Psi\rangle = |\Psi\rangle = P_{34}|\Psi\rangle$. Edge vortices σ_1 and σ_3 are fused at Josephson junction J_2 and vortices σ_2 and σ_4 are fused at junction J_4. The expectation value of the fermion parity upon fusion vanishes,

$$\begin{aligned} &\langle\Psi|P_{13}|\Psi\rangle = \langle\Psi|P_{12}P_{13}P_{12}|\Psi\rangle = -\langle\Psi|P_{13}P_{12}^2|\Psi\rangle = -\langle\Psi|P_{13}|\Psi\rangle \\ &\Rightarrow \langle\Psi|P_{13}|\Psi\rangle = 0, \end{aligned} \tag{3.2.2}$$

and similarly $\langle\Psi|P_{24}|\Psi\rangle = 0$. So the fusion of edge vortices at J_2 and J_3 leaves the edge modes in an equal weight superposition of odd and even fermion parity. This presence of multiple fusion channels is a defining property of non-Abelian anyons [3, 112, 113].

Because the overall fermion parity is conserved, the fusion outcomes at J_2 and J_3 must have the same fermion parity — either even-even or odd-odd. In the next two sections we present an explicit calculation of the fermion parity, to demonstrate that an $h/2e$ voltage pulse produces a superposition of even-even and odd-odd fermion parity states with identical probabilities P_{00} and $P_{11} = 1 - P_{00}$.

3.3 Scattering formula for the fermion parity

3.3.1 Construction of the fermion parity operator

We focus on the geometry of Fig. 3.3, with incoming and outgoing modes in the left lead (labeled L) and in the right lead (R). We seek the expectation value

$$\rho_\pi \equiv \left\langle e^{i\pi\mathcal{N}} \right\rangle = P_{00} - P_{11}, \tag{3.3.1}$$

of the fermion parity operator $e^{i\pi\mathcal{N}}$, with $\mathcal{N}$ the particle number operator of outgoing modes in one of the two leads. We will take the left lead for definiteness. In terms of the annilation operators $b_n(E)$ of outgoing modes n at excitation energy $E > 0$ this operator takes the form

$$\mathcal{N} = \sum_{n\in \mathrm{L}} \sum_{E>0} b_n^\dagger(E) b_n(E), \tag{3.3.2}$$

where we have discretized the energy. In the continuum limit $\sum_E \mapsto \int dE/2\pi$ and the Kronecker delta becomes a Dirac delta function, $\delta_{EE'} \mapsto 2\pi\delta(E - E')$.

Incoming and outgoing modes are related by a unitary scattering matrix,

$$b_n(E) = \sum_{m,E'} S_{nm}(E,E')a_m(E'), \tag{3.3.3}$$

$$\sum_{n'',E''} S^*_{n''n}(E'',E)S_{n''m}(E'',E') = \delta_{nm}\delta_{EE'}. \tag{3.3.4}$$

Note that the sums in these two equations run over positive and negative energies. Particle-hole symmetry relates

$$S_{nm}(-E,-E') = S^*_{nm}(E,E'). \tag{3.3.5}$$

We write Eq. (3.3.3) more compactly as $\boldsymbol{b} = \boldsymbol{S}\cdot\boldsymbol{a}$, collecting the mode and energy variables in vectors $\boldsymbol{a}$ and $\boldsymbol{b}$. The unitarity relation (3.3.4) is then written as $\boldsymbol{S}^\dagger\boldsymbol{S} = 1$. In terms of a projection operator $\mathcal{P}_\mathrm{L}$ onto modes in lead L, and a projection operator $\mathcal{P}_+$ onto positive energies, the combination of Eqs. (3.3.2) and (3.3.3) reads

$$\mathcal{N} = \boldsymbol{a}^\dagger\cdot\boldsymbol{M}\cdot\boldsymbol{a}, \quad \boldsymbol{M} = \boldsymbol{S}^\dagger\mathcal{P}_\mathrm{L}\mathcal{P}_+\boldsymbol{S}. \tag{3.3.6}$$

The expectation value $\langle\cdots\rangle = \mathrm{Tr}\,(\rho_\mathrm{eq}\cdots)$ is with respect to an equilibrium distribution of the incoming modes,

$$\rho_\mathrm{eq} \propto \exp\left(-\beta\sum_n\sum_{E>0} Ea^\dagger_n(E)a_n(E)\right). \tag{3.3.7}$$

We denote $\beta = 1/k_\mathrm{B}T$ and have omitted the normalization constant (fixed by $\mathrm{Tr}\,\rho_\mathrm{eq} = 1$).

The combination of particle-hole symmetry,

$$a^\dagger_n(E) = a_n(-E), \tag{3.3.8}$$

with anticommutation,

$$\{a^\dagger_n(E), a_m(E')\} = \delta_{nm}\delta_{EE'}, \tag{3.3.9}$$

allows us to extend the sum $\sum_{E>0}$ in Eq. (3.3.7) to a sum over positive and negative energies,

$$\rho_\mathrm{eq} \propto \exp\left(-\tfrac{1}{2}\beta\sum_{n,E} Ea^\dagger_n(E)a_n(E)\right) \equiv e^{-\frac{1}{2}\beta\boldsymbol{a}^\dagger\cdot\boldsymbol{E}\cdot\boldsymbol{a}}. \tag{3.3.10}$$

In the second equation we introduced the diagonal operator $\boldsymbol{E}_{nm}(E,E') = E\delta_{nm}\delta_{EE'}$.

With this notation the average fermion parity is given by the ratio of two operator traces,

$$\rho_\pi = \frac{\operatorname{Tr}\left(e^{-\frac{1}{2}\beta \boldsymbol{a}^\dagger\cdot\boldsymbol{E}\cdot\boldsymbol{a}} e^{i\pi \boldsymbol{a}^\dagger\cdot\boldsymbol{M}\cdot\boldsymbol{a}}\right)}{\operatorname{Tr} e^{-\frac{1}{2}\beta \boldsymbol{a}^\dagger\cdot\boldsymbol{E}\cdot\boldsymbol{a}}}. \tag{3.3.11}$$

3.3.2 Klich formula for particle-hole conjugate Majorana operators

Fermionic operator traces of the form (3.3.11) have been studied by Klich and collaborators [120–122]. For Dirac fermion creation and annihilation operators $\boldsymbol{d}^\dagger, \boldsymbol{d}$ one has the simple expression [120]

$$\operatorname{Tr} \prod_k e^{\boldsymbol{d}^\dagger\cdot\boldsymbol{O}_k\cdot\boldsymbol{d}} = \operatorname{Det}\left(1 + \prod_k e^{\boldsymbol{O}_k}\right). \tag{3.3.12}$$

The answer is different for self-conjugate Majorana operators $\boldsymbol{\gamma} = \boldsymbol{\gamma}^\dagger$, with anticommutator $\{\gamma_n, \gamma_m\} = \delta_{nm}$, when one has instead [122]

$$\left[\operatorname{Tr} \prod_k e^{\boldsymbol{\gamma}^\dagger\cdot\boldsymbol{O}_k\cdot\boldsymbol{\gamma}}\right]^2 = e^{\sum_k \operatorname{Tr}\boldsymbol{O}_k} \operatorname{Det}\left(1 + \prod_k e^{\boldsymbol{O}_k - \boldsymbol{O}_k^{\mathrm{T}}}\right). \tag{3.3.13}$$

(The superscript T indicates the transpose of the matrix.)

The Majorana fermion modes in the topological superconductor are not self-conjugate, instead creation and annihilation operators $\boldsymbol{a}^\dagger, \boldsymbol{a}$ are related by the particle-hole symmetry relation (3.3.8). In view of Eq. (3.3.9) this implies that annihilation operators at energies $\pm E$ fail to anticommute:

$$\{a_n(E), a_m(-E')\} = \delta_{nm}\delta_{EE'}. \tag{3.3.14}$$

This unusual anticommutator expresses the Majorana nature of Bogoliubov quasiparticles [123].

To arrive at the analogue of Eq. (3.3.13) for particle-hole conjugate Majorana operators we rewrite the bilinear form $\boldsymbol{a}^\dagger\cdot\boldsymbol{O}\cdot\boldsymbol{a}$ such that the $\boldsymbol{a}, \boldsymbol{a}^\dagger$ operators appear only at positive energies:

$$\begin{aligned}\boldsymbol{a}^\dagger\cdot\boldsymbol{O}\cdot\boldsymbol{a} &= \sum_{n,m}\sum_{E,E'} a_n^\dagger(E) O_{nm}(E,E') a_m(E') \\ &= \sum_{n,m}\sum_{E,E'>0} \begin{pmatrix} a_n^\dagger(E) \\ a_n(E)\end{pmatrix} \mathcal{O}_{nm}(E,E') \begin{pmatrix} a_m(E') \\ a_m^\dagger(E')\end{pmatrix}.\end{aligned} \tag{3.3.15}$$

The matrix $\mathcal{O}$ imposes on $\boldsymbol{O}$ a 2×2 block structure,

$$\mathcal{O} = \begin{pmatrix} \boldsymbol{O}_{++} & \boldsymbol{O}_{+-} \\ \boldsymbol{O}_{-+} & \boldsymbol{O}_{--} \end{pmatrix}, \tag{3.3.16}$$

to encode the sign of the energy variables:

$$(\boldsymbol{O}_{ss'})_{nm}(E,' E') = O_{nm}(sE, s'E') \text{ for } s, s' \in \{+,-\} \text{ and } E, E' > 0. \tag{3.3.17}$$

We introduce the 2×2 Pauli matrix σ_x that acts on the block structure of $\mathcal{O}$ and define the generalized antisymmetrization

$$\begin{aligned} \mathcal{O}^{\mathrm{A}} &= \tfrac{1}{2}\mathcal{O} - \tfrac{1}{2}\sigma_x \mathcal{O}^{\mathrm{T}} \sigma_x \\ &= \frac{1}{2}\begin{pmatrix} \boldsymbol{O}_{++} - \boldsymbol{O}_{--}^{\mathrm{T}} & \boldsymbol{O}_{+-} - \boldsymbol{O}_{+-}^{\mathrm{T}} \\ \boldsymbol{O}_{-+} - \boldsymbol{O}_{-+}^{\mathrm{T}} & \boldsymbol{O}_{--} - \boldsymbol{O}_{++}^{\mathrm{T}} \end{pmatrix}. \end{aligned} \tag{3.3.18}$$

Only $\mathcal{O}^{\mathrm{A}}$ and $\operatorname{Tr}\mathcal{O} = \operatorname{Tr}\boldsymbol{O}$ contribute to the Majorana fermion operator trace,

$$\left[\operatorname{Tr}\prod_k e^{\boldsymbol{a}^\dagger \cdot \boldsymbol{O}_k \cdot \boldsymbol{a}}\right]^2 = e^{\sum_k \operatorname{Tr}\boldsymbol{O}_k} \operatorname{Det}\left(1 + \prod_k e^{2\mathcal{O}_k^{\mathrm{A}}}\right), \tag{3.3.19}$$

see App. 3.B. Eq. (3.3.19) is the desired analogue of Eq. (3.3.13) for particle-hole conjugate Majorana operators.

3.3.3 Fermion parity as the determinant of a scattering matrix product

For the average fermion parity ρ_π we apply Eq. (3.3.19) to the ratio of operator traces (3.3.11). We start from the block decomposition of $\boldsymbol{E}, \boldsymbol{S}$, and $\boldsymbol{M} = \boldsymbol{S}^\dagger \mathcal{P}_{\mathrm{L}} \mathcal{P}_+ \boldsymbol{S}$,

$$\begin{aligned} &\mathcal{E} = \begin{pmatrix} \boldsymbol{E} & 0 \\ 0 & -\boldsymbol{E} \end{pmatrix} = \boldsymbol{E}\sigma_z, \quad \mathcal{S} = \begin{pmatrix} \boldsymbol{S}_{++} & \boldsymbol{S}_{+-} \\ \boldsymbol{S}_{-+} & \boldsymbol{S}_{--} \end{pmatrix}, \\ &\mathcal{M} = \tfrac{1}{2}\mathcal{S}^\dagger \mathcal{P}_{\mathrm{L}}(\sigma_0 + \sigma_z)\mathcal{S}. \end{aligned} \tag{3.3.20}$$

In the equation for $\mathcal{M}$ we substituted $\mathcal{P}_+ = \frac{1}{2}(\sigma_0 + \sigma_z)$, with σ_0 the 2×2 unit matrix.

The antisymmetrization of $\mathcal{E}$ is simple,

$$\mathcal{E}^{\mathrm{A}} \equiv \tfrac{1}{2}\mathcal{E} - \tfrac{1}{2}\sigma_x \mathcal{E}^{\mathrm{T}} \sigma_x = \boldsymbol{E}\sigma_z. \tag{3.3.21}$$

For the antisymmetrization of $\mathcal{M}$ we note that Eq. (3.3.5) implies $\sigma_x \mathcal{S} \sigma_x = \mathcal{S}^*$, hence

$$\sigma_x \mathcal{S}^{\mathrm{T}} \sigma_x = \mathcal{S}^\dagger \Rightarrow \mathcal{M}^{\mathrm{A}} = \tfrac{1}{2} \mathcal{S}^\dagger \mathcal{P}_{\mathrm{L}} \sigma_z \mathcal{S}. \tag{3.3.22}$$

We thus arrive at

$$\rho_\pi^2 = e^{i\pi \operatorname{Tr} \boldsymbol{M}} \frac{\operatorname{Det}\left(1 + e^{-\beta \boldsymbol{E} \sigma_z} e^{i\pi \mathcal{S}^\dagger \mathcal{P}_{\mathrm{L}} \sigma_z \mathcal{S}}\right)}{\operatorname{Det}\left(1 + e^{-\beta \boldsymbol{E} \sigma_z}\right)}. \tag{3.3.23}$$

The ratio of determinants is equivalent to a single determinant,

$$\begin{aligned} &\rho_\pi^2 = e^{i\pi \operatorname{Tr} \boldsymbol{M}} \operatorname{Det}\left(1 - \mathcal{F} + \mathcal{F} e^{i\pi \mathcal{S}^\dagger \mathcal{P}_{\mathrm{L}} \sigma_z \mathcal{S}}\right), \\ &\mathcal{F} = (1 + e^{\beta \boldsymbol{E} \sigma_z})^{-1}, \;\; 1 - \mathcal{F} = (1 + e^{-\beta \boldsymbol{E} \sigma_z})^{-1}. \end{aligned} \tag{3.3.24}$$

To proceed we first rewrite the exponent of the trace of $\boldsymbol{M}$ as a determinant,

$$e^{i\pi \operatorname{Tr} \boldsymbol{M}} = e^{i\pi \operatorname{Tr} \mathcal{P}_{\mathrm{L}} \mathcal{P}_+} \tag{3.3.25a}$$

$$= \operatorname{Det}\left[-\sigma_z\right]_{\mathrm{LL}} = \operatorname{Det}\left[\sigma_z\right]_{\mathrm{LL}} \;\text{ with }\; \sigma_z \equiv 2\mathcal{P}_+ - 1, \tag{3.3.25b}$$

$$= \operatorname{Det}\left[-\tau_z\right]_{++} = \operatorname{Det}\left[\tau_z\right]_{++} \;\text{ with }\; \tau_z \equiv 2\mathcal{P}_{\mathrm{L}} - 1. \tag{3.3.25c}$$

The notation $[\cdots]_{\mathrm{LL}}$ indicates a projection onto mode indices in the left lead, and $[\cdots]_{++}$ indicates a projection onto positive energies.

We then evaluate the exponent of the scattering matrix product,

$$\begin{aligned} &e^{i\xi \mathcal{S}^\dagger \mathcal{P}_{\mathrm{L}} \sigma_z \mathcal{S}} = \sigma_0 + i(\sin\xi) \mathcal{S}^\dagger \mathcal{P}_{\mathrm{L}} \sigma_z \mathcal{S} + (\cos\xi - 1) \mathcal{S}^\dagger \mathcal{P}_{\mathrm{L}} \mathcal{S}, \\ &\Rightarrow e^{i\pi \mathcal{S}^\dagger \mathcal{P}_{\mathrm{L}} \sigma_z \mathcal{S}} = \sigma_0 - 2\mathcal{S}^\dagger \mathcal{P}_{\mathrm{L}} \mathcal{S}, \end{aligned} \tag{3.3.26}$$

since $(\mathcal{S}^\dagger \mathcal{P}_{\mathrm{L}} \sigma_z \mathcal{S})^{2n} = \mathcal{S}^\dagger \mathcal{P}_{\mathrm{L}} \mathcal{S}$ and $(\mathcal{S}^\dagger \mathcal{P}_{\mathrm{L}} \sigma_z \mathcal{S})^{2n-1} = \mathcal{S}^\dagger \mathcal{P}_{\mathrm{L}} \sigma_z \mathcal{S}$, for $n = 1, 2, 3, \ldots$. It follows that

$$\rho_\pi^2 = e^{i\pi \operatorname{Tr} \boldsymbol{M}} \operatorname{Det}\left(1 - 2\mathcal{F} \mathcal{S}^\dagger \mathcal{P}_{\mathrm{L}} \mathcal{S}\right) \tag{3.3.27a}$$

$$= e^{i\pi \operatorname{Tr} \boldsymbol{M}} \operatorname{Det}\left(1 - 2\mathcal{P}_{\mathrm{L}} \mathcal{S} \mathcal{F} \mathcal{S}^\dagger\right) \tag{3.3.27b}$$

$$= e^{i\pi \operatorname{Tr} \boldsymbol{M}} \operatorname{Det}\left[1 - 2\mathcal{S} \mathcal{F} \mathcal{S}^\dagger\right]_{\mathrm{LL}} \tag{3.3.27c}$$

$$= \operatorname{Det}\left[\sigma_z\right]_{\mathrm{LL}} \operatorname{Det}\left[\mathcal{S}(1 - 2\mathcal{F}) \mathcal{S}^\dagger\right]_{\mathrm{LL}} \tag{3.3.27d}$$

$$= \operatorname{Det}\left[\sigma_z \mathcal{S} \tanh(\tfrac{1}{2}\beta \mathcal{E}) \mathcal{S}^\dagger\right]_{\mathrm{LL}}. \tag{3.3.27e}$$

In Eq. (3.3.27b) we used the Sylvester identity $\operatorname{Det}(1 - AB) = \operatorname{Det}(1 - BA)$, in Eq. (3.3.27c) we used $\operatorname{Det}(1 - \mathcal{P}_{\mathrm{L}} A) = \operatorname{Det}[1 - A]_{\mathrm{LL}}$, in Eq. (3.3.27d)

we used $\mathcal{S}\mathcal{S}^\dagger = 1$, and in (3.3.27e) we used that $\mathrm{Det}\,[A]_{\mathrm{LL}}\mathrm{Det}\,[B]_{\mathrm{LL}} = \mathrm{Det}\,[AB]_{\mathrm{LL}}$ if A or B commutes with $\mathcal{P}_{\mathrm{L}}$.

In what follows we restrict ourselves to zero temperature, when $\mathcal{F} \mapsto \mathcal{P}_-$ projects onto negative energies and $\tanh(\frac{1}{2}\beta\mathcal{E}) \mapsto \sigma_z$. Eq. (3.3.27e) then reduces to

$$\rho_\pi^2 = \mathrm{Det}\left[\sigma_z \mathcal{S} \sigma_z \mathcal{S}^\dagger\right]_{\mathrm{LL}}, \tag{3.3.28}$$

the determinant of a scattering matrix product projected onto mode indices in the left lead. An alternative projection onto positive energies is possible:

$$\begin{aligned}
\rho_\pi^2 &= e^{i\pi\,\mathrm{Tr}\,\boldsymbol{M}}\mathrm{Det}\left(1 - 2\mathcal{P}_-\mathcal{S}^\dagger\mathcal{P}_{\mathrm{L}}\mathcal{S}\right) && \text{(3.3.29a)}\\
&= e^{i\pi\,\mathrm{Tr}\,\boldsymbol{M}}\mathrm{Det}\left(1 - 2\mathcal{P}_+\mathcal{S}^\dagger\mathcal{P}_{\mathrm{L}}\mathcal{S}\right) && \text{(3.3.29b)}\\
&= \mathrm{Det}\,[-\tau_z]_{++}\,\mathrm{Det}\big[\mathcal{S}^\dagger(1 - 2\mathcal{P}_{\mathrm{L}})\mathcal{S}\big]_{++}, && \text{(3.3.29c)}
\end{aligned}$$

(In Eq. (3.3.29b) we used particle-hole symmetry, $\mathcal{S} = \sigma_x\mathcal{S}^*\sigma_x$, and $\sigma_x\mathcal{P}_-\sigma_x = \mathcal{P}_+$.) Because τ_z commutes with $\mathcal{P}_+$, Eq. (3.3.29c) may be combined into a a single determinant,

$$\rho_\pi^2 = \mathrm{Det}\big[\tau_z\mathcal{S}^\dagger\tau_z\mathcal{S}\big]_{++}. \tag{3.3.30}$$

Equations (3.3.28) and (3.3.30) express the average fermion parity of a scattering state as the determinant of a product of scattering matrices projected onto a submatrix in mode space, Eq. (3.3.28), or in energy space, Eq. (3.3.30).* Both equations give the square ρ_π^2 rather than ρ_π itself. Since we wish to show that $\rho_\pi = 0$, that is not a limitation for the present study.

3.3.4 Simplification in the adiabatic regime

The energy dependence of the scattering matrix is characterized by the inverse of two time scales of the Josephson junction: the dwell time $\tau_{\mathrm{dwell}} \simeq L/v_{\mathrm{F}}$ in the superconducting island and the characteristic time scale

$$t_\phi = (\xi_0/W)(d\phi/dt)^{-1} \tag{3.3.31}$$

for the variation of the superconducting phase shift. (The time t_ϕ is the "vortex injection time" t_{inj} of Ref. [116].) While $S(E, E')$ depends on the

*To avoid a possible confusion we note that, because of the projection, the product rule $\mathrm{Det}\,(AB) = (\mathrm{Det}\,A)(\mathrm{Det}\,B)$ cannot be applied to $\mathrm{Det}[AB]_{++}$ or $\mathrm{Det}[AB]_{\mathrm{LL}}$, unless A or B commutes with the projector.

average energy $\bar{E} = (E + E')/2$ on the scale $1/\tau_{\rm dwell}$, it depends on the energy difference $\delta E = E - E'$ on the scale $1/\tau_\phi$.

In the adiabatic regime $\tau_{\rm dwell} \ll \tau_\phi$ the scattering matrix $S(E, E')$ for $\bar{E} \lesssim 1/\tau_\phi \ll 1/\tau_{\rm dwell}$ is only a function of δE,

$$S(E, E') = \int_{-\infty}^{\infty} dt\, e^{i(E-E')t} S_{\rm F}(t) + \mathcal{O}(\tau_{\rm dwell}/\tau_\phi). \tag{3.3.32}$$

The unitary matrix $S_{\rm F}(t)$ is the "frozen" scattering matrix at the Fermi level, calculated for a fixed value $\phi \equiv \phi(t)$ of the superconducting phase.

The fermion parity determinant can be simplified in the adiabatic regime, because only energies within $1/\tau_\phi$ from the Fermi level contribute. This is most easily seen from Eq. (3.3.28), which is the determinant of the scattering matrix product $\Omega = \sigma_z \mathcal{S} \sigma_z \mathcal{S}^\dagger$, projected onto the left lead. A matrix element of Ω,

$$\Omega_{nm}(E, E') = (\operatorname{sign} E) \sum_{n', E''} (\operatorname{sign} E'') S_{nn'}(E, E'') S^*_{mn'}(E', E'') \tag{3.3.33}$$

is only nonzero for $|E - E'| \lesssim 1/\tau_\phi$. Moreover, $\Omega_{nm}(E, E') \approx \delta_{nm}\delta_{EE'}$ for $|E| \gtrsim 1/\tau_\phi$. Hence the determinant of Ω is fully determined by energies in the range $-1/\tau_\phi \lesssim E, E' \lesssim 1/\tau_\phi$, where $S(E, E')$ may be approximated by the frozen scattering matrix (3.3.32).

For computational purposes it is more convenient to rewrite the determinant (3.3.28) in the form (3.3.30), because the scattering matrix product $\tau_z \mathcal{S} \tau_z \mathcal{S}^\dagger$ is a convolution in energy space when $S(E, E')$ is a function of $E - E'$. The convolution is readily evaluated in the time domain, resulting in an expression for the fermion parity

$$\rho_\pi^2 = \operatorname{Det} [Q]_{++}, \tag{3.3.34}$$

in terms of the determinant of the projection onto $E, E' > 0$ of the matrix

$$Q(E, E') = \int_{-\infty}^{\infty} dt\, e^{i(E-E')t} Q(t), \quad Q(t) = \tau_z S_{\rm F}^\dagger(t) \tau_z S_{\rm F}(t). \tag{3.3.35}$$

In the next section we shall show how to evaluate this determinant.

3.4 Vanishing of the average fermion parity

We apply the formalism that we developed in Sec. 3.3 to the four-terminal Josephson junction of Sec. 3.2, in order to demonstrate that the 2π phase

shift produces a state with an equal weight $P_{00} = P_{11}$ of even-even and odd-odd fermion parity in the left and right leads. We work in the adiabatic regime, when $\rho_\pi = P_{00} - P_{11}$ is given by Eqs. 3.3.34 and (3.3.35) in terms of the "frozen" scattering matrix $S_\mathrm{F}(t)$, for a fixed phase $\phi(t)$.

3.4.1 Frozen scattering matrix of the Josephson junction

The frozen scattering matrix $S_\mathrm{F} \in \mathrm{SO}(4)$ is calculated in App. 3.A, resulting in

$$S_\mathrm{F} = \begin{pmatrix} e^{-i\alpha_4\nu_y} & 0 \\ 0 & e^{-i\alpha_2\nu_y} \end{pmatrix} \cdot \Pi \cdot \begin{pmatrix} e^{i\alpha_1\nu_y} & 0 \\ 0 & e^{i\alpha_3\nu_y} \end{pmatrix}, \quad \Pi = \begin{pmatrix} 0 & 0 & 1 & 0 \\ 0 & -1 & 0 & 0 \\ 1 & 0 & 0 & 0 \\ 0 & 0 & 0 & 1 \end{pmatrix}. \tag{3.4.1}$$

The Pauli matrix ν_y acts on the two Majorana modes in each lead. The scattering phase α_n depends on the superconducting phase difference ϕ through the relation [116]

$$\alpha_n = \arccos\left(\frac{\cos(\phi/2) + \tanh\beta_n}{1 + \cos(\phi/2)\tanh\beta_n}\right) \times \mathrm{sign}\,(\phi), \quad \beta_n = \frac{W_n}{\xi_0}\cos(\phi/2). \tag{3.4.2}$$

A 2π increment of ϕ corresponds to a π increment of α_n, irrespective of the width W_n of the Josephson junction or the superconducting coherence length $\xi_0 = \hbar v_\mathrm{F}/\Delta_0$.

We need to evaluate the matrix product $\tau_z S_\mathrm{F}^\dagger \tau_z S_\mathrm{F}$, where the Pauli matrix

$$\tau_z = \begin{pmatrix} 1 & 0 & 0 & 0 \\ 0 & 1 & 0 & 0 \\ 0 & 0 & -1 & 0 \\ 0 & 0 & 0 & -1 \end{pmatrix} \tag{3.4.3}$$

is defined with respect to the block structure of modes in the left and right lead. Because of the identity

$$\Pi\tau_z\Pi = \begin{pmatrix} \nu_z & 0 \\ 0 & \nu_z \end{pmatrix}, \tag{3.4.4}$$

this matrix product is block-diagonal,

$$Q(t) = \tau_z S_\mathrm{F}^\dagger(t)\tau_z S_\mathrm{F}(t) = -\begin{pmatrix} \nu_z e^{2i\nu_y\alpha_1(t)} & 0 \\ 0 & \nu_z e^{2i\nu_y\alpha_3(t)} \end{pmatrix}, \tag{3.4.5}$$

independent of α_2 and α_4.

3.4.2 Reduction of the fermion parity to a Toeplitz determinant

Instead of taking a single 2π phase increment it is more convenient to assume a sequence of 2π phase shifts with period Δt. Then $\alpha_n(t)$ varies periodically in time with $\alpha_n(t+\Delta t) = \pi + \alpha_n(t)$. We Fourier transform to the energy domain,

$$\begin{aligned} \boldsymbol{T}_n(k,k') &= \frac{1}{\Delta t}\int_0^{\Delta t} dt\, e^{2\pi i(k-k')t/\Delta t} e^{2i\alpha_n(t)\nu_y}, \\ T_n(k,k') &= \frac{1}{\Delta t}\int_0^{\Delta t} dt\, e^{2\pi i(k-k')t/\Delta t} e^{2i\alpha_n(t)}, \end{aligned} \tag{3.4.6}$$

and restrict $k, k' \in \{1, 2, 3, \ldots\}$ to positive integers. The infinite matrix $T_n(k,k')$ has constant diagonals, so it is a Toeplitz matrix. Eq. (3.3.30) becomes the product of Toeplitz determinants,

$$\rho_\pi^2 = (\mathrm{Det}\,\boldsymbol{T}_1)(\mathrm{Det}\,\boldsymbol{T}_3) = |\mathrm{Det}\,T_1|^2\,|\mathrm{Det}\,T_3|^2. \tag{3.4.7}$$

The Toeplitz matrices T_n are banded matrices which extend over a large number of order W/ξ_0 of diagonals around the main diagonal. This follows from the fact that the π increment of $\alpha(t)$ happens in the time interval $t_\phi = (\xi_0/W)(\Delta t/2\pi)$ which is much shorter than Δt for $\xi_0 \ll W$. The ratio $t_\phi/\Delta t$ governs the exponential decay of the Toeplitz matrix elements as one moves away from the main diagonal, according to

$$|T_n(k,k')| \simeq \exp(-c_{\mathrm{decay}}|k-k'|), \quad c_{\mathrm{decay}} = \frac{\pi^2 t_\phi}{\Delta t} = \frac{\pi\xi_0}{2W}. \tag{3.4.8}$$

3.4.3 Fisher-Hartwig asymptotics

In a general formulation, the function $b(\theta)$ defines the $K \times K$ Toeplitz matrix

$$B_K(k,k') = \int_0^{2\pi} e^{i(k-k')\theta} b(\theta)\,\frac{d\theta}{2\pi}, \quad k,k' \in \{1,2,\ldots K\}. \tag{3.4.9}$$

If b is smooth and nonvanishing on the unit circle $0 < \theta < 2\pi$, it has a well-defined winding number

$$\nu = \frac{1}{2\pi i}\int_0^{2\pi} \frac{b'(\theta)}{b(\theta)}\,d\theta. \tag{3.4.10}$$

The number ν may be non-integer, or even complex, if b has a jump discontinuity at $\theta = 0$.

The Fisher-Hartwig asymptotics [124, 125] determines the large-K limit of the determinant of B_K from the decomposition $b(\theta) = b_0(\theta)e^{i\nu\theta}$, where b_0 has zero winding number. In the most general case the function b_0 may have (integrable) singularities, but if we assume it is smooth the asymptotics reads

$$\begin{aligned} \operatorname{Det} B_K \simeq & \exp\left(\frac{K}{2\pi}\int_0^{2\pi} \ln b_0(\theta)\, d\theta\right) \\ & \times \begin{cases} K^{-\nu^2} & \text{for non-integer } \nu, \\ e^{-|\nu| c_{\mathrm{decay}} K} & \text{for integer } \nu. \end{cases} \end{aligned} \tag{3.4.11}$$

The coefficient c_{decay} in the exponent is the decay rate $|B_K(k,k')| \simeq \exp(-c_{\mathrm{decay}}|k-k'|)$ of the Toeplitz matrix elements as we move away from the diagonal.

Applied to $b(t) = e^{2i\alpha(t)}$, $\theta = 2\pi t/\Delta t$, we have $\nu = 1$, $b_0(t) = e^{2i\alpha(t)-2\pi i t/\Delta t}$. The Toeplitz determinant

$$\operatorname{Det} B_K \simeq e^{-c_{\mathrm{decay}} K} \exp\left(\frac{2iK}{\Delta t}\int_0^{\Delta t} \alpha(t)dt - i\pi K\right) \tag{3.4.12}$$

vanishes exponentially in the limit $K \to \infty$, with decay rate $c_{\mathrm{decay}} = \pi\xi_0/W$ determined by the ratio of the superconducting coherence length ξ_0 and the width W of the Josephson junction.

For the evaluation of the fermion parity, the band width $K/\Delta t$ is limited by the energy range $|\bar{E}| \lesssim 1/t_{\mathrm{dwell}}$ where the dependence of the scattering matrix $S(E,E')$ on the average energy $\bar{E} = (E+E')/2$ may be neglected. We thus conclude that

$$\begin{aligned} |\rho_\pi| \simeq \exp(-2c_{\mathrm{decay}}K) &\simeq \exp\left(-\frac{2\pi\xi_0}{W}\frac{\Delta t}{t_{\mathrm{dwell}}}\right) \\ &\simeq \exp\left(-\frac{4\pi^2 t_\phi}{t_{\mathrm{dwell}}}\right), \end{aligned} \tag{3.4.13}$$

which is exponentially small in the adiabatic regime $t_\phi \gg t_{\mathrm{dwell}}$.

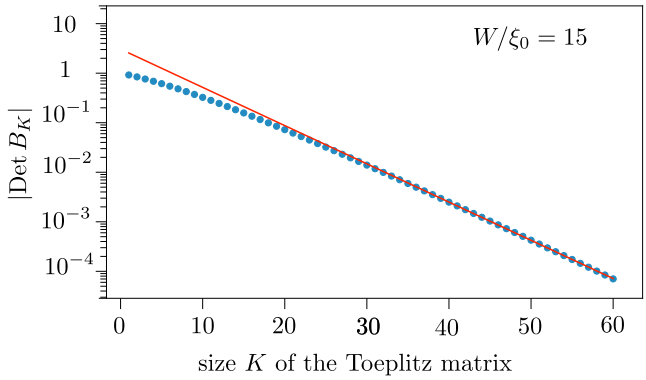

Figure 3.4: Decay of the Toeplitz determinant (data points), compared with the exponential decay expected from Eq. (3.4.12). The constant c_{decay} was calculated separately from $|B_K(k,k')| \simeq \exp(-c_{\mathrm{decay}}|k-k'|)$. The estimate $c_{\mathrm{decay}} = \pi\xi_0/W$ is off by 15%.

3.5 Transferred charge

3.5.1 Average charge

The average charge $\langle Q_{\mathrm{L}}\rangle$, $\langle Q_{\mathrm{R}}\rangle$ transferred into the left or right lead during one 2π increment of ϕ is given, in the adiabatic regime, by the superconducting analogue of Brouwer's formula [106, 107]:

$$\begin{aligned}\langle Q_{\mathrm{L}}\rangle &= \frac{ie}{4\pi}\int_{-\infty}^{\infty} dt\,\mathrm{Tr}\, S_{\mathrm{F}}^{\dagger}(t)\begin{pmatrix}\nu_y & 0\\ 0 & 0\end{pmatrix}\frac{\partial}{\partial t}S_{\mathrm{F}}(t),\\ \langle Q_{\mathrm{R}}\rangle &= \frac{ie}{4\pi}\int_{-\infty}^{\infty} dt\,\mathrm{Tr}\, S_{\mathrm{F}}^{\dagger}(t)\begin{pmatrix}0 & 0\\ 0 & \nu_y\end{pmatrix}\frac{\partial}{\partial t}S_{\mathrm{F}}(t).\end{aligned} \tag{3.5.1}$$

Substitution of Eq. (3.4.1) gives

$$\begin{aligned}\langle Q_{\mathrm{L}}\rangle &= \frac{e}{2\pi}\int_{-\infty}^{\infty} dt\,\frac{d}{dt}\alpha_4(t),\\ \langle Q_{\mathrm{R}}\rangle &= \frac{e}{2\pi}\int_{-\infty}^{\infty} dt\,\frac{d}{dt}\alpha_2(t).\end{aligned} \tag{3.5.2}$$

Because both α_2 and α_4 increase by π when ϕ is incremented by 2π, see Eq. (3.4.2), we conclude that

$$\langle Q_{\mathrm{L}}\rangle = \langle Q_{\mathrm{R}}\rangle = \frac{e}{2}. \tag{3.5.3}$$

While the average transferred charge per cycle is exactly $e/2$, the average particle number is close to but not exactly equal to $1/2$ — indicating that there is a small contribution from charge-neutral particle-hole pairs.*

3.5.2 Charge correlations

Fluctuations in the transferred charge are described by the second moments $\langle Q_{\rm L}^2\rangle$, $\langle Q_{\rm R}^2\rangle$, and $\langle Q_{\rm L}Q_{\rm R}\rangle$. Scattering matrix formulas for these correlators are derived in App. 3.C. In the adiabatic regime one has

$$\mathrm{var}(Q_{\rm L}) \equiv \langle Q_{\rm L}^2\rangle - \langle Q_{\rm L}\rangle^2 = \frac{e^2}{8\pi^2}\int_{0^+}^{\infty} d\omega\,\omega\,\mathrm{Tr}\,\Sigma_{\rm L}^\dagger(\omega)\Sigma_{\rm L}(\omega), \tag{3.5.4a}$$

$$\mathrm{var}(Q_{\rm R}) \equiv \langle Q_{\rm R}^2\rangle - \langle Q_{\rm R}\rangle^2 = \frac{e^2}{8\pi^2}\int_{0^+}^{\infty} d\omega\,\omega\,\mathrm{Tr}\,\Sigma_{\rm R}^\dagger(\omega)\Sigma_{\rm R}(\omega), \tag{3.5.4b}$$

$$\begin{aligned}\mathrm{covar}(Q_{\rm L}Q_{\rm R}) &\equiv \tfrac{1}{2}\langle Q_{\rm L}Q_{\rm R}\rangle + \tfrac{1}{2}\langle Q_{\rm R}Q_{\rm L}\rangle - \langle Q_{\rm L}\rangle\langle Q_{\rm R}\rangle \\ &= \frac{e^2}{16\pi^2}\int_{0^+}^{\infty} d\omega\,\omega\,\mathrm{Tr}\,\left[\Sigma_{\rm L}^\dagger(\omega)\Sigma_{\rm R}(\omega) + \Sigma_{\rm R}^\dagger(\omega)\Sigma_{\rm L}(\omega)\right],\end{aligned} \tag{3.5.4c}$$

in terms of the matrices

$$\Sigma_{\rm L}(\omega) = \int_{-\infty}^{\infty} dt\, e^{i\omega t}\,\Sigma_{\rm L}(t),\quad \Sigma_{\rm L}(t) = S_{\rm F}^\dagger(t)\begin{pmatrix}\nu_y & 0\\ 0 & 0\end{pmatrix} S_{\rm F}(t), \tag{3.5.5a}$$

$$\Sigma_{\rm R}(\omega) = \int_{-\infty}^{\infty} dt\, e^{i\omega t}\,\Sigma_{\rm R}(t),\quad \Sigma_{\rm R}(t) = S_{\rm F}^\dagger(t)\begin{pmatrix}0 & 0\\ 0 & \nu_y\end{pmatrix} S_{\rm F}(t). \tag{3.5.5b}$$

The lower limit 0^+ in the ω-integrals (3.5.4) avoids a spurious contribution $\propto \delta(\omega)$.

From the expression (3.4.1) for $S_{\rm F}(t)$ we find

$$\begin{aligned}\mathrm{Tr}\,\Sigma_{\rm L}^\dagger(\omega)\Sigma_{\rm L}(\omega) &= \mathrm{Tr}\,\Sigma_{\rm R}^\dagger(\omega)\Sigma_{\rm R}(\omega)\\ &= \tfrac{1}{2}|Z_+(\omega)|^2 + \tfrac{1}{2}|Z_+(-\omega)|^2 + \tfrac{1}{2}|Z_-(\omega)|^2 + \tfrac{1}{2}|Z_-(-\omega)|^2,\end{aligned} \tag{3.5.6a}$$

$$\begin{aligned}\mathrm{Tr}\,\Sigma_{\rm L}^\dagger(\omega)\Sigma_{\rm R}(\omega) &= \mathrm{Tr}\,\Sigma_{\rm R}^\dagger(\omega)\Sigma_{\rm L}(\omega)\\ &= \tfrac{1}{2}|Z_+(\omega)|^2 + \tfrac{1}{2}|Z_+(-\omega)|^2 - \tfrac{1}{2}|Z_-(\omega)|^2 - \tfrac{1}{2}|Z_-(-\omega)|^2,\end{aligned} \tag{3.5.6b}$$

$$Z_\pm(\omega) = \int_{-\infty}^{\infty} dt\, e^{i\omega t} e^{i\alpha_1(t)\pm i\alpha_3(t)}. \tag{3.5.6c}$$

*A calculation along the lines of Ref. [116] of the average number of quasiparticles transferred per cycle into the left or the right lead gives $\langle N_{\rm L}\rangle = \langle N_{\rm R}\rangle = 42\zeta(3)/\pi^4 = 0.518$.

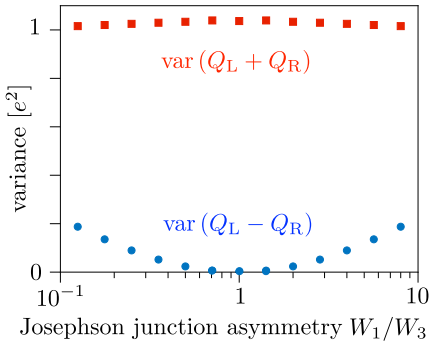

Figure 3.5: Variance of the sum and difference of the transferred charges upon fusion of the edge vortices in Josephson junctions J_2 and J_4, as a function of the asymmetry in the width of the injecting Josephson junctions J_1 and J_3.

The dependence on α_2 and α_4 drops out.

Without further calculation we see that for $\alpha_1 = \alpha_3$ the contribution of $Z_-(\omega)$ to the correlators (3.5.4) vanishes, hence $\mathrm{covar}(Q_\mathrm{L}Q_\mathrm{R}) = \mathrm{var}(Q_\mathrm{L}) = \mathrm{var}(Q_\mathrm{R})$. This implies that the charge difference $Q_\mathrm{L} - Q_\mathrm{R}$ is zero without fluctuations,

$$\mathrm{var}\,(Q_\mathrm{L} - Q_\mathrm{R}) = \mathrm{var}\,(Q_\mathrm{L}) + \mathrm{var}\,(Q_\mathrm{R}) - 2\,\mathrm{covar}(Q_\mathrm{L}Q_\mathrm{R}) = 0. \tag{3.5.7}$$

The charges Q_L and Q_R do fluctuate individually, with a variance close to $e^2/4$, and so does the sum $Q_\mathrm{L} + Q_\mathrm{R}$, with a variance close to e^2. These values can be calculated precisely for the time dependence [116]

$$\alpha(t) \approx \arccos\left[\tanh\left(\frac{W}{\xi_0}\frac{\pi - \phi(t)}{2}\right)\right] \approx \arccos[-\tanh(t/2t_\phi)], \tag{3.5.8}$$

which is an accurate representation of Eq. (3.4.2) for $W/\xi_0 \gg 1$. We find

$$Z_+(\omega) = 2\pi\delta(\omega) - \frac{8\pi\omega t_\phi^2}{\sinh(\pi\omega t_\phi)} + \frac{8\pi\omega t_\phi^2}{\cosh(\pi\omega t_\phi)}, \quad Z_-(\omega) = 2\pi\delta(\omega), \tag{3.5.9}$$

$$\Rightarrow \mathrm{var}\,(Q_\mathrm{L}) = \mathrm{var}\,(Q_\mathrm{R}) = \tfrac{1}{4}\mathrm{var}\,(Q_\mathrm{L} + Q_\mathrm{R}) = \frac{21\zeta(3)}{\pi^4}\,e^2 = 0.259\,e^2. \tag{3.5.10}$$

For $\alpha_1 \neq \alpha_3$ we can evaluate the integrals numerically using the time dependence

$$\alpha_n = \arccos\left[-\tanh(t/2t_n)\right], \tag{3.5.11}$$

increasing from 0 to π in a time $t_n = (\xi_0/W_n)(\Delta t/2\pi)$ around $t = 0$. Results for var $(Q_\mathrm{L} \pm Q_\mathrm{R})$ are shown in Fig. 3.5. The shot noise for the charge difference remains suppressed for a moderately large deviation from unity of W_1/W_3.

3.6 Conclusion

We have shown how the method of time-resolved and "on-demand" injection of edge vortices proposed in Ref. [116] can be used to demonstrate the non-Abelian fusion rule of Majorana zero-modes. The signature of the correlated but non-deterministic outcome of the fusion of two pairs of edge vortices is a fluctuating electrical current I_L and I_R through two Josephson junctions, induced by a 2π phase shift of the pair potential. While the sum $I_\mathrm{L} + I_\mathrm{R}$ has average e per cycle and variance close to e^2, the difference $I_\mathrm{L} - I_\mathrm{R}$ vanishes without fluctuations in a symmetric structure (and remains much below e^2 for moderate asymmetries).

The four-terminal structure of chiral Majorana edge modes that we have studied has been investigated before in the context of the injection of fermions [33, 117–119]. A Majorana fermion that splits into partial waves at opposite edges defines a nonlocally encoded *charge qubit*: a coherent superposition of an electron and a hole.* In contrast, the injection of vortices at opposite edges is a nonlocal encoding of the *fermion parity*. The difference could be significant for quantum information processing if the fermion parity qubit is more robust against decoherence than the charge qubit. We surmise that zero-modes in edge vortices are better protected against charge noise and other local sources of decoherence than Majorana fermions — basically because a Majorana fermion is charge neutral on average but does exhibit quantum fluctuations of the charge.

Much further research is needed to substantiate the potential of edge vortices as carriers of quantum information, but we feel that they have much to offer at least for the demonstration of basic operations in topological quantum computation: the braiding operation of Ref. [116] and the non-deterministic fusion operation considered here.

*The splitting of a Majorana fermion into partial waves does not provide a local encoding of the fermion parity because a measurement at one edge can detect the presence or absence of a fermion.

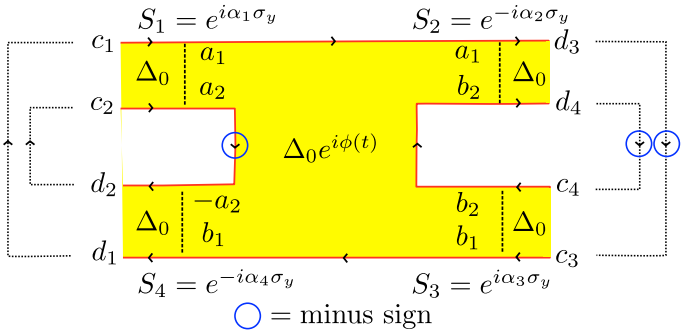

Figure 3.6: Labeling of incoming and outgoing Majorana edge modes in a four-terminal Josephson junction.

3.A Calculation of the frozen scattering matrix

Consider first the stationary scattering problem, when the four-terminal Josephson junction from Fig. 3.3 has a time-independent phase difference ϕ. This gives the "frozen" scattering matrix $S_{\mathrm{F}}(E, \phi)$, which we evaluate at the Fermi level ($E = 0$).

As calculated in Ref. [116], each of the four terminals (width W_n) has at the Fermi level a scattering matrix in SO(2) given by

$$\begin{aligned} S_n &= \begin{pmatrix} \cos\alpha_n & \sin\alpha_n \\ -\sin\alpha_n & \cos\alpha_n \end{pmatrix} = e^{i\alpha_n\nu_y} \quad \text{for} \quad n = 1, 3, \\ S_n &= \begin{pmatrix} \cos\alpha_n & -\sin\alpha_n \\ \sin\alpha_n & \cos\alpha_n \end{pmatrix} = e^{-i\alpha_n\nu_y} \quad \text{for} \quad n = 2, 4. \end{aligned} \tag{3.A.1}$$

The Pauli matrix ν_y acts on the two Majorana modes at a Josephson junction. The angles α_n are given as a function of ϕ and the ratio W_n/ξ_0 by Eq. (3.4.2) from the main text.

Referring to the labeling of modes from Fig. 3.6, we have the linear

relations

$$\begin{pmatrix} d_1 \\ d_2 \\ d_3 \\ d_4 \end{pmatrix} = S_{\mathrm{F}} \begin{pmatrix} c_1 \\ c_2 \\ c_3 \\ c_4 \end{pmatrix}, \tag{3.A.2a}$$

$$\begin{pmatrix} a_1 \\ a_2 \end{pmatrix} = S_1 \begin{pmatrix} c_1 \\ c_2 \end{pmatrix}, \quad \begin{pmatrix} d_3 \\ d_4 \end{pmatrix} = S_2 \begin{pmatrix} a_1 \\ b_2 \end{pmatrix},$$

$$\begin{pmatrix} b_1 \\ b_2 \end{pmatrix} = S_3 \begin{pmatrix} c_3 \\ c_4 \end{pmatrix}, \quad \begin{pmatrix} d_1 \\ d_2 \end{pmatrix} = S_4 \begin{pmatrix} b_1 \\ -a_2 \end{pmatrix}. \tag{3.A.2b}$$

The minus sign for the coefficient a_2 in the last equality accounts for the π Berry phase of a circulating Majorana edge mode. As indicated by the dotted lines in Fig. 3.6, the edge modes are segments of three closed loops. We choose a gauge where the minus sign in each loop is acquired on the downward branch, indicated by the blue circle. This only affects the branch with amplitude a_2, because the other two downward branches are outside of the scattering region.

Elimination of the a_n and b_n variables gives

$$S_{\mathrm{F}} = \begin{pmatrix} -\sin\alpha_1 \sin\alpha_4 & \cos\alpha_1 \sin\alpha_4 & \cos\alpha_3 \cos\alpha_4 & \cos\alpha_4 \sin\alpha_3 \\ \cos\alpha_4 \sin\alpha_1 & -\cos\alpha_1 \cos\alpha_4 & \cos\alpha_3 \sin\alpha_4 & \sin\alpha_3 \sin\alpha_4 \\ \cos\alpha_1 \cos\alpha_2 & \cos\alpha_2 \sin\alpha_1 & \sin\alpha_2 \sin\alpha_3 & -\cos\alpha_3 \sin\alpha_2 \\ \cos\alpha_1 \sin\alpha_2 & \sin\alpha_1 \sin\alpha_2 & -\cos\alpha_2 \sin\alpha_3 & \cos\alpha_2 \cos\alpha_3, \end{pmatrix}, \tag{3.A.3}$$

which may be written more compactly as Eq. (3.4.1). One can check that $S_{\mathrm{F}} \in \mathrm{SO}(4)$, in particular, it has determinant $+1$ as it should be in the absence of a Majorana zero-mode [126].*

In the adiabatic regime the scattering matrix $S(E, E')$ of the time-dependent problem is related to the frozen scattering matrix $S_{\mathrm{F}}(E, \phi)$ via

$$S(E + \tfrac{1}{2}\omega, E - \tfrac{1}{2}\omega) \approx \int_{-\infty}^{\infty} dt\, e^{i\omega t} S_{\mathrm{F}}(E, \phi(t)). \tag{3.A.4}$$

Near the Fermi level we may furthermore neglect the dependence on the average energy, approximating

$$S(E, E') \approx \int_{-\infty}^{\infty} dt\, e^{i(E-E')t} S_{\mathrm{F}}(0, \phi(t)). \tag{3.A.5}$$

*If we would not have accounted for the sign change of a_2 the determinant of S_{F} would have been -1.

3.B Derivation of the Klich formula

The operator trace (3.3.19) for particle-hole conjugate Majorana operators $a(E) = a^\dagger(-E)$ can be derived from the Klich formula (3.3.13) for self-conjugate Majorana operators $\gamma = \gamma^\dagger$, by performing a unitary transformation:

$$\begin{pmatrix}\gamma_n(E)\\ \gamma'_n(E)\end{pmatrix} = U \begin{pmatrix}a_n(E)\\ a_n^\dagger(E)\end{pmatrix}, \quad U = \frac{1}{\sqrt{2}}\begin{pmatrix}1 & 1\\ -i & i\end{pmatrix}. \tag{3.B.1}$$

At positive energies the γ operators satisfy the Clifford algebra of Majorana operators,

$$\begin{aligned}\{\gamma_n(E),\gamma_m(E')\} &= \{\gamma'_n(E),\gamma'_m(E')\}\\ &= \{\gamma_n(E),\gamma'_m(E')\} = \delta_{nm}\delta_{EE'}, \quad E,E'>0.\end{aligned} \tag{3.B.2}$$

Note that

$$\gamma_n(E)^2 = \gamma'_n(E)^2 = 1/2. \tag{3.B.3}$$

The bilinear form (3.3.15) of the a operators transforms into

$$\boldsymbol{a}^\dagger \cdot \boldsymbol{O} \cdot \boldsymbol{a} = \sum_{n,m}\sum_{E,E'>0} \begin{pmatrix}\gamma_n(E)\\ \gamma'_n(E)\end{pmatrix} \tilde{\mathcal{O}}_{nm}(E,E') \begin{pmatrix}\gamma_m(E')\\ \gamma'_m(E')\end{pmatrix}, \tag{3.B.4}$$

with $\tilde{\mathcal{O}} = U\mathcal{O}U^\dagger$. Because only positive energies appear in Eq. (3.B.4), we may apply the anticommutator (3.B.2), which implies that the traceless symmetric part of $\tilde{\mathcal{O}}$ drops out. Only the trace $\operatorname{Tr}\tilde{\mathcal{O}} = \operatorname{Tr}\mathcal{O}$ and the antisymmetric part $(\tilde{\mathcal{O}} - \tilde{\mathcal{O}}^{\mathrm{T}})/2$ contribute,

$$\boldsymbol{a}^\dagger \cdot \boldsymbol{O} \cdot \boldsymbol{a} = \tfrac{1}{2}\boldsymbol{\gamma}\cdot(\tilde{\mathcal{O}} - \tilde{\mathcal{O}}^{\mathrm{T}})\cdot\boldsymbol{\gamma} + \tfrac{1}{2}\operatorname{Tr}\boldsymbol{O}. \tag{3.B.5}$$

After these preparations we can apply Klich's original formula [122],

$$\begin{aligned}\left[\operatorname{Tr}\prod_k \exp(\boldsymbol{a}^\dagger\cdot\boldsymbol{O}_k\cdot\boldsymbol{a})\right]^2 &= \exp\left(\sum_k \operatorname{Tr}\boldsymbol{O}_k\right)\\ &\quad\times \operatorname{Det}\left(1+\prod_k \exp(\tilde{\mathcal{O}}_k - \tilde{\mathcal{O}}_k^{\mathrm{T}})\right).\end{aligned} \tag{3.B.6}$$

Finally we invert the unitary transformation,

$$U^\dagger\tilde{\mathcal{O}}U = \mathcal{O}, \quad U^\dagger\tilde{\mathcal{O}}^T U = (U^{\mathrm{T}}U)^\dagger\mathcal{O}^{\mathrm{T}}(U^{\mathrm{T}}U) = \sigma_x\mathcal{O}^{\mathrm{T}}\sigma_x, \tag{3.B.7}$$

to arrive at

$$\left[\operatorname{Tr}\prod_k \exp(\boldsymbol{a}^\dagger\cdot\boldsymbol{O}_k\cdot\boldsymbol{a})\right]^2 = \exp\left(\sum_k \operatorname{Tr}\boldsymbol{O}_k\right) \times \operatorname{Det}\left(1+\prod_k \exp(\mathcal{O}_k-\sigma_x\mathcal{O}_k^{\mathrm{T}}\sigma_x)\right), \tag{3.B.8}$$

which is Eq. (3.3.19).

3.C Scattering formulas for charge correlators

3.C.1 General expressions for first and second moments

Moments of the transferred charge in the left lead are given by the expectation value

$$\langle Q_{\mathrm{L}}^p\rangle = \left\langle \left(\boldsymbol{a}^\dagger\cdot\boldsymbol{Q}\cdot\boldsymbol{a}\right)^p\right\rangle, \quad \boldsymbol{Q}=\boldsymbol{S}^\dagger\mathcal{P}_{\mathrm{L}}\mathcal{P}_+ e\nu_y\boldsymbol{S}. \tag{3.C.1}$$

In comparison with the number operator (3.3.6) there is a matrix $e\nu_y$ which is the charge operator in the Majorana basis. (It would be $e\nu_z$ in the particle-hole basis.) The expectation value $\langle\cdots\rangle = \operatorname{Tr}(\rho_{\mathrm{eq}}\cdots)$ is with respect to an equilibrium distribution of the $\boldsymbol{a}$ operators, with density matrix (3.3.7).

Because of the Majorana commutator (3.3.14), we have both the usual type-I average

$$\langle a_n^\dagger(E)a_m(E')\rangle = \delta_{nm}\delta(E-E')f(E), \quad f(E)=(1+e^{\beta E})^{-1}, \tag{3.C.2}$$

and the unusual type-II average

$$\langle a_n(E)a_m(E')\rangle = \delta_{nm}\delta(E+E')f(-E), \quad f(-E)=1-f(E). \tag{3.C.3}$$

Averages of strings of a and $a^\dagger$ operators are obtained by summing over all pairwise averages of both types I and II, signed by the permutation.*

*An equivalent procedure [123] is to first use the relation $a_n(-E)=a_n^\dagger(E)$ to rewrite the expectation value such that only positive energies appear, and then apply Wick's theorem as usual.

We assume zero temperature, when $f(E) = \mathcal{P}_-$ and $1 - f(E) = \mathcal{P}_+$ are step functions of energy.

The first moment of the transferred charge contains a single type-I average,

$$\langle Q_{\rm L} \rangle = \operatorname{Tr} \mathcal{P}_- \boldsymbol{Q} = \int_0^\infty \frac{dE}{2\pi} \int_{-\infty}^0 \frac{dE'}{2\pi} \operatorname{Tr} S^\dagger(E, E') e\nu_y \mathcal{P}_{\rm L} S(E, E'). \tag{3.C.4}$$

The variance contains a term with two type-I averages and a term with two type-II averages,

$$\begin{aligned} \operatorname{var}(Q_{\rm L}) = {} & \operatorname{Tr} \mathcal{P}_- \boldsymbol{Q} \mathcal{P}_+ \boldsymbol{Q} \\ & - \int_0^\infty \frac{dE}{2\pi} \int_{-\infty}^0 \frac{dE'}{2\pi} \sum_{n,m} Q_{nm}(-E, -E') Q_{nm}(E, E'). \end{aligned} \tag{3.C.5}$$

The particle-hole symmetry relation (3.3.5) of the scattering matrix implies that

$$Q_{nm}(-E, -E') = -(\boldsymbol{S}^\dagger \mathcal{P}_{\rm L} \mathcal{P}_- e\nu_y \boldsymbol{S})_{mn}(E', E). \tag{3.C.6}$$

Substitution into Eq. (3.C.5) gives

$$\operatorname{var}(Q_{\rm L}) = \operatorname{Tr} \mathcal{P}_- \boldsymbol{Q} \mathcal{P}_+ \boldsymbol{Q} + \operatorname{Tr} \mathcal{P}_- \boldsymbol{Q}' \mathcal{P}_+ \boldsymbol{Q}, \tag{3.C.7}$$

with $\boldsymbol{Q}'$ as in Eq. (3.C.1) upon replacement of $\mathcal{P}_+$ by $\mathcal{P}_-$. Since $\mathcal{P}_+ + \mathcal{P}_- = 1$, this reduces to

$$\operatorname{var}(Q_{\rm L}) = \operatorname{Tr} \mathcal{P}_- (\boldsymbol{S}^\dagger \mathcal{P}_{\rm L} e\nu_y \boldsymbol{S}) \mathcal{P}_+ (\boldsymbol{S}^\dagger \mathcal{P}_{\rm L} \mathcal{P}_+ e\nu_y \boldsymbol{S}). \tag{3.C.8}$$

It is convenient to eliminate the second $\mathcal{P}_+$ projector from Eq. (3.C.8). This can be done via particle-hole symmetry, which implies that

$$\begin{aligned} & \operatorname{Tr} \mathcal{P}_- (\boldsymbol{S}^\dagger \mathcal{P}_{\rm L} e\nu_y \boldsymbol{S}) \mathcal{P}_+ (\boldsymbol{S}^\dagger \mathcal{P}_{\rm L} \mathcal{P}_+ e\nu_y \boldsymbol{S}) \\ & \qquad = \operatorname{Tr} (\boldsymbol{S}^\dagger \mathcal{P}_{\rm L} \mathcal{P}_+ e\nu_y \boldsymbol{S})^{\rm T} \mathcal{P}_+ (\boldsymbol{S}^\dagger \mathcal{P}_{\rm L} e\nu_y \boldsymbol{S})^{\rm T} \mathcal{P}_- \\ & \qquad = \operatorname{Tr} (\boldsymbol{S}^\dagger \mathcal{P}_{\rm L} \mathcal{P}_- e\nu_y \boldsymbol{S}) \mathcal{P}_- (\boldsymbol{S}^\dagger \mathcal{P}_{\rm L} e\nu_y \boldsymbol{S}) \mathcal{P}_+ \\ & \qquad = \operatorname{Tr} \mathcal{P}_- (\boldsymbol{S}^\dagger \mathcal{P}_{\rm L} e\nu_y \boldsymbol{S}) \mathcal{P}_+ (\boldsymbol{S}^\dagger \mathcal{P}_{\rm L} \mathcal{P}_- e\nu_y \boldsymbol{S}). \end{aligned} \tag{3.C.9}$$

Hence

$$\tfrac{1}{2} \operatorname{Tr} \mathcal{P}_- (\boldsymbol{S}^\dagger \mathcal{P}_{\rm L} e\nu_y \boldsymbol{S}) \mathcal{P}_+ (\boldsymbol{S}^\dagger \mathcal{P}_{\rm L} (\mathcal{P}_- - \mathcal{P}_+) e\nu_y \boldsymbol{S}) = 0, \tag{3.C.10}$$

and adding this to Eq. (3.C.8) we arrive at

$$\begin{aligned}\operatorname{var}(Q_{\mathrm{L}}) &= \frac{1}{2}\operatorname{Tr}\mathcal{P}_{-}(\boldsymbol{S}^{\dagger}\mathcal{P}_{\mathrm{L}}e\nu_y\boldsymbol{S})\mathcal{P}_{+}(\boldsymbol{S}^{\dagger}\mathcal{P}_{\mathrm{L}}e\nu_y\boldsymbol{S}) \\ &= \frac{1}{2}e^2\int_0^{\infty}\frac{dE}{2\pi}\int_{-\infty}^{0}\frac{dE'}{2\pi}\operatorname{Tr}\Sigma_{\mathrm{L}}^{\dagger}(E,E',)\Sigma_{\mathrm{L}}(E,E'), \qquad (3.\mathrm{C}.11) \\ \boldsymbol{\Sigma}_{\mathrm{L}} &= \boldsymbol{S}^{\dagger}\mathcal{P}_{\mathrm{L}}\nu_y\boldsymbol{S}.\end{aligned}$$

The expressions for the other correlators are analogous,

$$\operatorname{var}(Q_{\mathrm{R}}) = \frac{1}{2}e^2\int_0^{\infty}\frac{dE}{2\pi}\int_{-\infty}^{0}\frac{dE'}{2\pi}\operatorname{Tr}\Sigma_{\mathrm{R}}^{\dagger}(E,E')\Sigma_{\mathrm{R}}(E,E'), \qquad (3.\mathrm{C}.12)$$

$$\begin{aligned}\boldsymbol{\Sigma}_{\mathrm{R}} &= \boldsymbol{S}^{\dagger}\mathcal{P}_{\mathrm{R}}\nu_y\boldsymbol{S}, \\ \operatorname{covar}(Q_{\mathrm{L}}Q_{\mathrm{R}}) &= \frac{1}{4}e^2\int_0^{\infty}\frac{dE}{2\pi}\int_{-\infty}^{0}\frac{dE'}{2\pi}\operatorname{Tr}\Big[\Sigma_{\mathrm{L}}^{\dagger}(E,E')\Sigma_{\mathrm{R}}(E,E') \\ &\quad + \Sigma_{\mathrm{R}}^{\dagger}(E,E')\Sigma_{\mathrm{L}}(E,E')\Big]. \qquad (3.\mathrm{C}.13)\end{aligned}$$

Eq. (3.C.13) gives the symmetrized covariance,

$$\operatorname{covar}(Q_{\mathrm{L}}Q_{\mathrm{R}}) \equiv \tfrac{1}{2}\langle Q_{\mathrm{L}}Q_{\mathrm{R}}\rangle + \tfrac{1}{2}\langle Q_{\mathrm{R}}Q_{\mathrm{L}}\rangle - \langle Q_{\mathrm{L}}\rangle\langle Q_{\mathrm{R}}\rangle, \qquad (3.\mathrm{C}.14)$$

appropriate for a calculation of $\operatorname{var}(Q_{\mathrm{L}} \pm Q_{\mathrm{R}})$.

3.C.2 Adiabatic approximation

The general expressions (3.C.4) and (3.C.11)–(3.C.13) can be simplified in the adiabatic regime, when near the Fermi level $S(E,E')$ depends only on the energy difference $\omega = E - E'$. We use the identity

$$\int_0^{\infty}dE\int_{-\infty}^{0}dE'\,F(E-E') = \int_{0^+}^{\infty}d\omega\,\omega F(\omega). \qquad (3.\mathrm{C}.15)$$

The lower integration limit 0^+ eliminates a possibly singular delta function in $F(\omega)$, which should not enter in the excitation spectrum.

For the average transferred charge (3.C.4) we thus have

$$\langle Q_{\mathrm{L}}\rangle = \frac{1}{4\pi^2}\int_{0^+}^{\infty}d\omega\,\omega\operatorname{Tr}S^{\dagger}(\omega)e\nu_y\mathcal{P}_{\mathrm{L}}S(\omega). \qquad (3.\mathrm{C}.16)$$

As explained in Ref. [116], this is equivalent to the Brouwer formula (3.5.1): Because of

$$[S^\dagger(\omega)\nu_y\mathcal{P}_\mathrm{L}S(\omega)]^\mathrm{T} = -S^\dagger(-\omega)\nu_y\mathcal{P}_\mathrm{L}S(-\omega) \tag{3.C.17}$$

the integrand in Eq. (3.C.16) is an even function of ω, hence the integration can be extended to $\int_{-\infty}^{\infty} d\omega$, and then transformation to the time domain gives Eq. (3.5.1).

For the second moments we use that the kernels $\Sigma(E, E') \mapsto \Sigma(\omega)$ are functions of $\omega = E - E'$ when $S(E, E') \mapsto S(\omega)$,

$$\begin{aligned}
\Sigma_{\mathrm{L,R}}(E, E') &= \int_{-\infty}^{\infty} \frac{dE''}{2\pi}\, S^\dagger(E'', E)\mathcal{P}_{\mathrm{L,R}}\nu_y S(E'', E') \\
\Rightarrow \Sigma_{\mathrm{L,R}}(\omega) &= \int_{-\infty}^{\infty} \frac{d\omega'}{2\pi}\, S^\dagger(\omega' - \omega)\mathcal{P}_{\mathrm{L,R}}\nu_y S(\omega') \\
&= \int_{-\infty}^{\infty} dt\, e^{i\omega t} S^\dagger(t)\mathcal{P}_{\mathrm{L,R}}\nu_y S(t).
\end{aligned} \tag{3.C.18}$$

The Fourier transform is defined as

$$S(\omega) = \int_{-\infty}^{\infty} dt\, e^{i\omega t} S(t). \tag{3.C.19}$$

Note that for the representation (3.C.18) of $\Sigma(\omega)$ as a single time integral it was essential that we eliminated the $\mathcal{P}_+$ projector from the scattering matrix product.

Application of Eqs. (3.C.15) and (3.C.18) to Eqs. (3.C.11)–(3.C.13) then gives the formulas (3.5.4) from the main text.